Proceedings of ITC18,2008

First result on Z_{eff} Profile Analysis from Visible Bremsstrahlung Measurement for Different Density Profiles in LHD

Hangyu Zhou[1], Shigeru Morita[2], Motoshi Goto[2]

[1]*Department of Fusion Science, Graduate University for Advanced Studies,*

Toki 509-5292, Gifu, Japan

[2]*National Institute for Fusion Science, Toki 509-5292, Gifu, Japan*

Visible bremsstrahlung emission has been measured using a optimized Czerny-Turner spectrometer newly installed on LHD. The bremsstrahlung emission profile has been successfully observed in some limited discharge conditions having no asymmetric strong edge bremsstrahlung emissions which are originated in the ergodic layer. Z_{eff} profiles are analyzed for peaked, flat and hollow density profiles as the first trial of the analysis. As a result, a flat Z_{eff} profile is obtained for all different density profiles. It indicates that the partial impurity pressure is basically constant against the plasma radius.

Keywords: Z_{eff} profile, visible bremsstrahlung, density profile

1. Introduction

Fuel dilution and enhanced radiation loss caused by impurity buildup are still one of serious problems in magnetic confinement fusion research. Impurity transport study becomes therefore important for understanding the impurity behavior and for improving plasma performance [1,2]. In Large Helical Device (LHD), a variety of electron density profiles such as peaked, flat and hollow profiles have been observed in different experimental conditions, which are quite different from the density profile usually seen in tokamaks, i.e., peaked profile. It is very interesting to study the impurity transport in such different density profiles. For the purpose full-vertical Z_{eff} profiles have been measured in LHD to obtain important information necessary for the impurity transport study, especially in plasma core region.

Visible bremsstrahlung emission has been measured with an optimized Czerny-Turner visible spectrometer [3] newly installed on LHD The instrument can entirely eliminate line emissions from the bremsstrahlung signal, which was one of serious problems in old bremsstrahlung measurement system with interference filter [4]. The new visible spectrometer system consists of 44 fiber array, an astigmatism-corrected Czerny-Turner visible spectrometer and a charge-coupled device (CCD) with vertical spatial resolution of 2.6cm and time resolution of 100ms. However, an asymmetric bremsstrahlung profile has been still observed after changing the diagnostic system. As a result of detailed data analysis, it was found that the asymmetric part of the signal originates in edge bremsstrahlung emission from thick ergodic layer. Fortunately, we could confirm that the lower half of the vertical bremsstrahlung profile had no influence from the edge emission in inwardly shifted magnetic configurations (R_{ax}≤3.6m) where the ergodic layer thickness is relatively thin. The local bremsstrahlung emission is calculated from chord-integrated signals after Abel inversion using elliptical magnetic surface with finite-β effect. The Z_{eff} profile is finally obtained with considering electron density and temperature profiles measured by Thomson scattering diagnostic [5]. In this paper the Z_{eff} profiles from LHD are presented in different density profile cases.

2. Experimental setup

The Czerny-turner visible spectrometer consists of a toroidal mirror, a flat mirror, two spherical mirrors and three gratings. A short focal length of 300mm is adopted to achieve a highly bright system. The three gratings of 120 (blaze: 330nm), 300 (500nm) and 1200 (200nm) grooves/mm are set in the turret. In the usual LHD experiments, the 300 grooves/mm grating is mainly used to observe wider wavelength range of 500nm to 600nm with relatively higher spectral resolution. The brightness of the 300 grooves/mm was very similar to the 120 grooves/mm. Vertical fiber array (-0.6m≤z≤0.6m) is installed with parallel view chords at horizontally

author's e-mail: zhou.hangyu@nifs.ac.jp

elongated plasma cross-section of LHD. The fiber array consists of 44 quartz optical fibers with core diameter of 100μm and clad diameter of 125μm. The spatial resolution, e.g., 30mm at the plasma center, is defined by optical lens with focal length of 30mm, which is coupled with each optical fiber. The output spectra are detected by CCD. The CCD has detection area of 13.3 × 13.3 mm^2 (1024 × 1024 channels, 13 μm × 13 μm/pixel). It is generally operated at -20°C to reduce the thermal noise. Exposure time of 31ms and temporal resolution of 100ms are selected in the present study with readout speed of 11 μs/line and 0.4 μs/pixel.

3. Analysis of radial Z_{eff} profile

Density profiles in LHD basically changes according to heating power, magnetic field strength, magnetic axis position and fuel method.

The peaked density profile is easily produced by hydrogen multi-pellets injection. The Z_{eff} profile is analyzed for the peak density profile formed in high-density range with the pellet injection. A typical waveform of such a discharge is traced in Fig.1. Ten H_2 pellets are repetitively injected in magnetic axis of 3.85m during 1.70-2.02s. Plasma energy quickly increases during pellet injection and reaches 0.9MJ. Line-averaged electron density evaluated from density profile measured with Thomson scattering continuously increases and reaches $3.5\times10^{14}cm^{-3}$, whereas electron temperature in the plasma center dramatically decreases down to 0.3keV. Chord-integrated bremsstrahlung emission also increases in the same way as density behavior and reaches a quite large value of $490\mu Wcm^{-2}nm^{-1}$. The β value is largely increased and becomes 1.13%. At 1.822s after the third pellet injection, the radial Z_{eff} profile is analyzed with electron density and temperature profiles in addition to local bremsstrahlung emissivity after Abel inversion. It is shown in Fig.2. The temperature profile is entirely flat at ρ<0.8 and quickly decreases at ρ>0.8. The outside boundary of the edge temperature expands to ρ=1.2 in the ergodic layer. The bremsstrahlung emissivity profile is also peaked as density profile. The Z_{eff} profile analyzed from the peaked density profile is fairly flat at the core plasma region inside ρ=1.0. The values of Z_{eff} distribute around 1.13. In the ergodic layer, which is denoted with yellow square hatch in Fig.2, it is difficult to analyze the Z_{eff} because of large uncertainties in density and temperature profiles of Thomson scattering. Error bars of the Z_{eff} profile basically originated in the density and temperature profiles are considerably inside ρ= 0.7. However, it gradually increases at edge plasmas, e.g., 23% at ρ=1.0. The fitting curves for electron density and temperature profiles used in the present analysis are also indicated in Fig.2 (a) and (b). Another important point on uncertainty of the Z_{eff} profile is in the selection of magnetic surface deformed by plasma pressure. The magnetic surface is of course necessary for Abel inversion of the line-integrated bremsstrahlung signal.

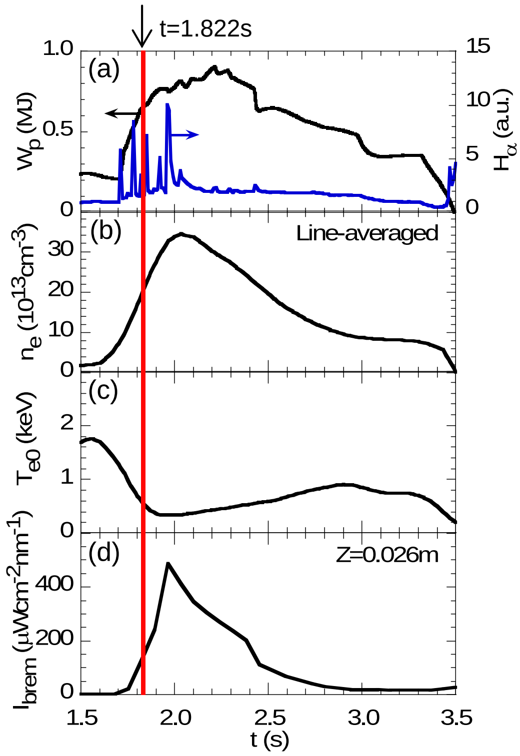

FIG.1 Waveform of high-density discharge with multi-pellets injection for peak density profile.

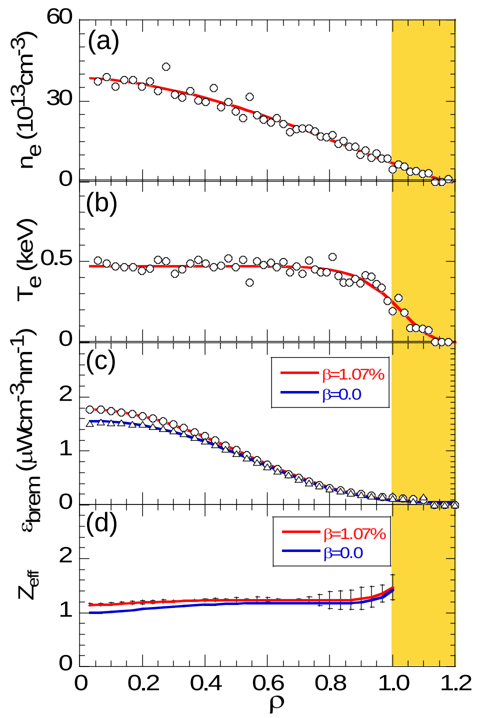

FIG.2 Profiles as a function of normalized radius at t=1.822s for multi-pellets injection discharge.

The uncertainty of the Z_{eff} profile due to magnetic surface deformation is checked using different two magnetic surfaces with β=0 and 1.07. Two bremsstrahlung emissivity profiles are obtained from the two magnetic surfaces, as shown in Fig.2 (c). The two bremsstrahlung emissivity profiles are quite similar, whereas a small difference is appeared in the plasma core. Since the visible bremsstrahlung is horizontally observed from outboard side of the torus, the effect on the magnetic surface distortion becomes much less compared to vertical measurement. Especially, the difference in the Z_{eff} value can be neglected at the outer plasma region, because the magnetic surface distortion is mainly occured in the plasma core. It is then strongly suggested that the uncertainty in the Z_{eff} profile on the assumed magnetic surface is quite small compared to that on the density and temperature profiles in the present diagnostic system.

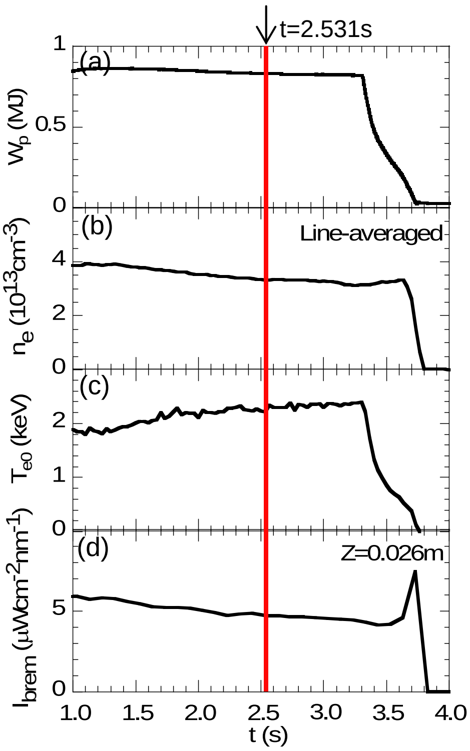

FIG.3 Time evolvement of stable discharge for flat density profile.

Next, the Z_{eff} profile is analyzed for flat density profile. The data are taken from stable plasma discharge in R_{ax}=3.6m. The discharge waveform is traced in Fig.3. The plasma energy is constantly sustained from 0.8s to 3.3s. The line-averaged electron density is roughly kept at $3.5\times10^{13}cm^{-3}$ and the central electron temperature slightly increases from 2.0keV to 2.2keV during the steady phase accroding to the gradual decrease in the density. The chord-integrated bremsstrahlung behaves similar to the desnity. The β value is 0.88% at the steady phase. The Zeff profile is calculated at 2.531s with electron density and temperature profiles as shown in Fig.2 (b). The density profile is entirely flat at ρ < 0.9, whereas the temperature profile is peaked. The bremsstrahlung emissivity profile after Abel inversion becomes a little hollow. This indicates small temperature dependence in the visible bremsstrahlung emission. The Z_{eff} profile is flat with values near 2.05. The analysis in the ergodic layer is still difficult. Error bars of the Z_{eff} profile gradually increase toward plasma core and the maximum error bar is appeared as 12% at the plasma center. It is clear that the error bars increased at the plasma core is originated in the local emissivity calculation of the bremsstrahlung based on Abel inversion method.

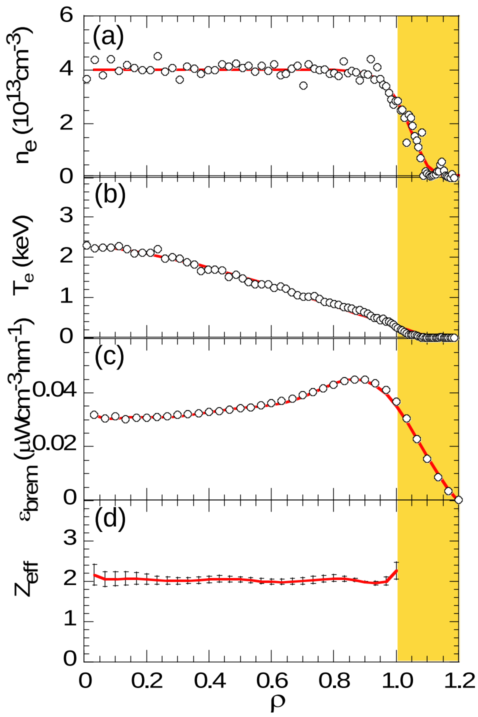

FIG.4 Radial profiles at t=2.531s produced by stable discharge.

Finally, the Z_{eff} profile is analyzed for hollow density profile. The hollow density profile is observed at density rise phase in R_{ax}=3.60m. The discharge waveform used in the analysis is shown in Fig.3 (a). The line-averaged electron density gradually increases during 0.5-1.5s and finally reaches $6\times10^{-13}cm^{-3}$, although the plasma energy is kept constant. The central plasma temperature then decreases from 1.8 to 1.2keV. The chord-integrated bremsstrahlung also increases according to the density rise. The β value is 0.88% in the discharge. At 2.531s, The Z_{eff} profile is analyzed at 2.531s. The electron density and temperature profiles are shown in Fig.3 (b) with local bremsstrahlung emissivity profile. The hollow density profile is formed having its peak value at ρ=0.9. On the contrary the

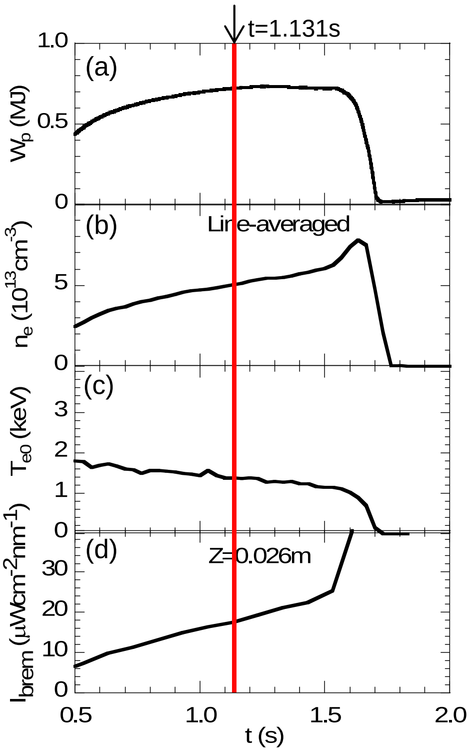

FIG.5 Trace of stable discharge for hollow density profile.

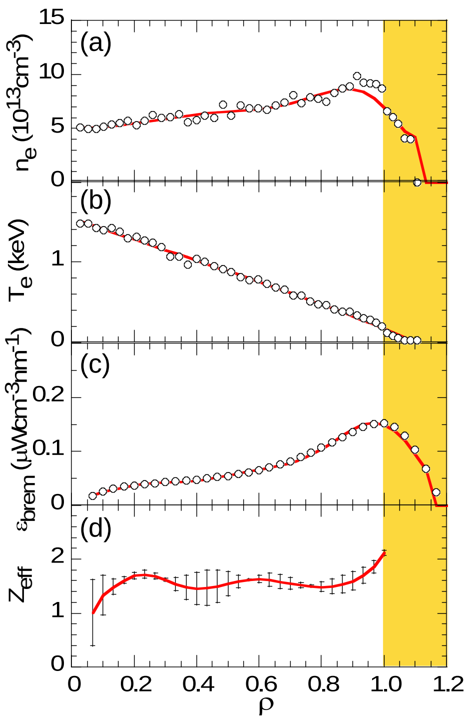

FIG.6 Profiles as a function of normalized radius at 1.131s during stable discharge.

temperature profile is peaked and forms a triangle shape.The bremsstrahlung emissivity largely decreases at the plasma core and the profile becomes much hollower than the density profile. The Z_{eff} profile is also flat with values around 1.58. In case of the hollow density profile, the analysis is generally difficult because of relatively large error bars in the density profile and difficulty in the Abel inversion calculation. The error bars in the Z_{eff} profile become also large in this case, i.e., ~20% at ρ = 0.4 and ~30% at plasma core. At present, any discussions can not be therefore done on the detailed structure in the Z_{eff} profile.

4. Summary and Discussion

Z_{eff} profile from visible bremsstrahlung measurement is analyzed for peaked, flat and hollow density profiles in LHD plasmas. The flat Z_{eff} profile is basically obtained for all different density profiles. It indicates that the impurity partial pressure is constant in general discharges of LHD. The error bars seen in the Z_{eff} profiles are mainly originated in fitting curves to express the electron temperature and density profiles and in process in the Abel inversion calculation. The uncertainty on magnetic surface distortion is relatively small. More precise Z_{eff} profile analysis will be done after optimizing the magnetic surface used in the calculation and modifying the method on Abel inversion calculation.

[1] D. P. Schissel et al., Phys. Fluids **31**, 3738 (1988).
[2] S. Morita, M.Goto et al., Physica Scripta T91, 48 (2001).
[3] H. Y. Zhou, S. Morita, M.Goto, M. B. Chowdhuri, Rev. Sci. Instrum. 79, 10F536 (2008)
[4] H. Nozato, S. Morita, M. Goto, J. Plasma Fusion Res. 5, 442 (2002)
[5] K.Nrihara et al., Rev. Sci. Instrum. 72, 1122 (2001)